Involvement of TMEM22 overexpression in the growth of renal cell carcinoma cells

SACHIKO DOBASHI[1], TOYOMASA KATAGIRI[1,5], EIJI HIROTA[1,2], SINGO ASHIDA[3], YATARO DAIGO[1], TARO SHUIN[3], TOMOAKI FUJIOKA[4], TSUNEHARU MIKI[2] and YUSUKE NAKAMURA[1]

[1]Laboratory of Molecular Medicine, Human Genome Center, Institute of Medical Science, The University of Tokyo, Tokyo 108-8639; [2]Department of Urology, Kyoto Prefectural University of Medicine, Kyoto 602-8566; [3]Department of Urology, Kochi Medical School, Kochi 783-8505; [4]Department of Urology, Iwate Medical University, Morioka 020-8505, Japan

Received June 25, 2008; Accepted August 11, 2008

DOI: 10.3892/or_00000222

Abstract. In order to clarify the molecular mechanism involved in renal carcinogenesis, and to identify molecular targets for development of novel treatments of renal cell carcinoma (RCC), we previously analyzed genome-wide gene expression profiles of clear-cell types of RCC by cDNA microarray. Among the transcativated genes, we herein focused on functional significance of *TMEM22* (transmembrane protein 22), a transmembrane protein, in cell growth of RCC. Northern blot and semi-quantitative RT-PCR analyses confirmed up-regulation of *TMEM22* in a great majority of RCC clinical samples and cell lines examined. Immunocytochemical analysis validated its localization at the plasma membrane. We found an interaction between TMEM22 and RAB37 (Ras-related protein Rab-37), which was also up-regulated in RCC cells. Interestingly, knockdown of either of TMEM22 or RAB37 expression by specific siRNA caused significant reduction of cancer cell growth. Our results imply that the TMEM22/RAB37 complex is likely to play a crucial role in growth of RCC and that inhibition of the TMEM22/RAB37 expression or their interaction should be novel therapeutic targets for RCC.

Introduction

Renal cell carcinoma (RCC) accounts for ~3% of all malignancies (1). At present, RCC at an early stage can be cured by surgical resection that is the most effective treatment for localized RCC tumors (2). Although immunotherapy is also available, the patients who obtained clinically meaningful benefit were very limited; for example, only 14% of the cases with metastatic RCC respond to a single treatment of interferon-α, and high-dose interleukin-2 (IL-2) treatment induce responses in only 21% of patients with advanced RCC (2). Moreover, these treatments can be associated with considerable toxicity (2,3). In order to overcome these disadvantages, recent molecular-targeting therapy, such as anti-VEGF antibody (bevacizumab), small molecule VEGFR inhibitors (sunitinib and sorafenib) have been developed and demonstrated to prolong survival in phase II and III trials (3-5). However, such treatments also showed limited anti-tumoral effects and various severe side effects beyond expectation (4,5). Therefore, development of a new molecular target drug(s) against RCC is earnestly desired.

Gene-expression profiles obtained by cDNA microarray analysis have been proven to provide detailed characterization of individual cancers and such information should contribute to improve clinical strategies for neoplastic diseases through development of novel drugs as well as providing the basis of personalized treatment (6). Through the genome-wide expression analysis we have isolated a number of genes that function as oncogenes in the process of development and/or progression of RCC (7,8), bladder cancer (9,10) and breast cancers (11-15). In an attempt to identify novel molecular targets for RCC therapy, we previously analyzed detailed gene-expression profiles of clinical clear cell type RCC (ccRCC), which is a major histological type of RCC, using a genome-wide cDNA microarray consisting of 27,648 genes or ESTs (8).

Among the up-regulated genes in ccRCC, we focused on *TMEM22*, which was highly overexpressed in the great majority of ccRCC cells examined. *TMEM22* was previously isolated as a candidate gene for glaucoma by expression profile analysis using primary culture human trabecular meshwork cells, and suspected to be a member of the drug metabolite transporter superfamily (16). However, its pathophysiological role and biological functions in cancer cells have not been reported.

Correspondence to: Dr Yusuke Nakamura, Laboratory of Molecular Medicine, Human Genome Center, Institute of Medical Science, The University of Tokyo, 4-6-1 Shirokanedai, Minato-ku, Tokyo 108-8639, Japan
E-mail: yusuke@ims.u-tokyo.ac.jp

Present address: [5]Division of Genome Medicine, Institute for Genome Research, The University of Tokushima, Tokushima 770-8503, Japan

Key words: cDNA microarray, molecular-target, membrane-protein

We herein report identification and characterization of TMEM22 as one of the key factors involved in renal carcinogenesis. We demonstrated the interaction of TMEM22 and RAB37 (Ras-related protein Rab-37), and knocking down either of them by their specific siRNAs leads to the significant growth suppression of RCC cells. Our findings suggest that TMEM22 may be a promising molecular target for RCC therapy through inhibition of the TMEM22/RAB37 expression or their interaction.

Materials and methods

RCC cell lines and tissue samples. The human renal cell carcinoma (RCC) cell lines, Caki-1, Caki-2, 786-O, A498, ACHN and 769-P were purchased from American Type Culture Collection (ATCC; Rockville, MD). OS-RC-2 was provided by the RIKEN BioResource Center (Tsukuba, Japan). VMRC-RCW was provided by the Cell Resource Center for Biomedical Research, Institute of Development, Aging and Cancer, Tohoku University. RXF-631L was a kind giftof Dr Takao Yamori, Division of Molecular Pharmacology, Cancer Chemotherapy Center, Japanese Foundation for Cancer Research. KMRC1, YCR, KC12 and KMRC20 were kind gifts of Dr Taro Shuin, Department of Urology, Kochi Medical School. All cells were grown in monolayers in appropriate medium supplemented with 10% fetal bovine serum (FBS) (Cansera International, Ontario, Canada) except ACHN (5%), and 1% antibiotic/ antimycotic solution (Sigma-Aldrich, St. Louis, MO). Cells were maintained at 37˚C in atmospheres of humidified air with 5% CO_2. Tissue samples of surgically-resected RCC and their corresponding clinical information were obtained from patients with written informed consent at three hospitals participating in this study, Juntendo University School of Medicine, Kochi Medical School and Kyoto Prefectural University of Medicine.

Semi-quantitative reverse transcription-PCR. We extracted total RNA from each of microdissected RCC clinical samples, microdissected normal renal cortex and cultured cells using RNeasy micro kits (Qiagen, Valencia, CA), and purchased polyA (+) RNAs isolated from heart, lung, liver and kidney (Takara Clontech, Kyoto, Japan) as described previously (8). Subsequently, we performed T7-based amplification and reverse transcription as described previously (8). We prepared appropriate dilutions of each single-stranded cDNA for subsequent PCR amplification and monitored their reactions using Farnesyl-diphosphate farnesyltransferase 1 (*FDFT1*) as a quantitative control because this showed the smallest Cy5/Cy3 fluctuations in our RCC-microarray data (8). The sequences of each set of primers were as follows; 5'-ATC CCATTAGATGGAGAAACCTG-3' and 5'-GTCCTGCTT TCTTAAATTCCTCC-3' for *TMEM22*; 5'-AGTGAAATG CAGGTGAGAAGAAC-3', and 5'-TCATTCTAGCCAGGA TCATACTAAG-3' for *FDFT1*. PCR reactions were optimized for the number of cycles to ensure product intensity within the logarithmic phase of amplification.

Northern blot analysis. Northern blot analysis for RCC cell-lines was prepared according to the procedures of our previous report (8). Northern blot analysis for RCC cell-lines were hybridized for 16 h with α^{32}P-labeled PCR product of *TMEM22* cDNA. The cDNA probes of *TMEM22* were prepared by RT-PCR using the primer set used for semi-quantitative RT-PCR as described above. Labeling, pre-hybridization, hybridization and washing were performed according to the previous report (17). The blots were auto-radiographed with intensifying screens at -80˚C for 14 days.

Construction of expression vectors. To construct TMEM22 expression vector, the entire coding sequences of TMEM22 cDNA was amplified by the PCR using KOD-Plus DNA polymerase (Toyobo, Osaka, Japan). The primer sets used for PCR reactions were as follows; TMEM22-forward; 5'-GGAATTCATGGATACTTCTCCCTCCAG-3' (the underline indicates *EcoR*I site) and TMEM22-reverse; 5'-CCTCGAGTTTAATGGGAGAGTCTAGTA-3' (the underline indicates *Xho*I site). Each PCR product was inserted into the *EcoR*I and *Xho*I sites of pCAGGSnH3F expression vector, pCAGGSnHC or pCAGGSn3FC. The pCAGGSnHC-RAB37 and pCAGGSn3FC-RAB37 plasmids were prepared previously (Y. Daigo and Y. Nakamura, unpublished data).

Anti-TMEM22 specific polyclonal antibody. A cDNA fragment of encoding N-terminus extracellular domain (4-103 amino acid residues) of TMEM22 was amplified by the PCR, and then subcloned into the pET28b vector (Merck, Novagen, Darmstadt, Germany). The primer set was 5'-GGAATTCGTCTCCCTCCAGAAAATATC-3' and 5'-CCGCTCGAGTTTTCGGGATTGAAAAATG-3' (underlines indicate the recognition sites of restriction enzymes). The recombinant peptide was expressed in *Escherichia coli*, BL21 codon-plus strain (Stratagene, La Jolla, CA, USA), and purified using Ni-NTA resin agarose (Qiagen) according to the supplier's protocols. The purified recombinant protein was used for immunization of rabbits (Medical and Biological Laboratories, Nagoya, Japan). Subsequently, the immune serum was purified on antigen affinity columns using Affi-gel 10 gel (Bio-Rad, Hercules, CA, USA) according to supplier's instructions. We confirmed that this antibody could specifically recognize the exogenously expressed TMEM22 protein by Western blot analysis.

Western blot analysis. Cells were lysed in membrane protein-lysis buffer [50 mM Tris-HCl/150mM NaCl/1 mM CHAPS/0.1% (w/v) digitonin], including 0.1% protease inhibitor cocktail III (Calbiochem, San Diego, CA). After homogenization, the cell lysates were incubated on ice for 30 min and centrifuged at 14,000 rpm for 15 min to separate only supernatant from cell debris. The amount of total protein was estimated by DC protein assay kit (Bio-Rad), and the proteins were then mixed with SDS sample buffer and incubated at 37˚C for 15 min before loading into a 12% SDS-PAGE gel. After electrophoresis, the proteins were transferred onto nitrocellulose membrane (GE Healthcare, Buckinghamshire, UK). Membranes were blocked by 4% Block Ace (Dainippon Pharmaceutical, Osaka, Japan), and incubated with anti-TMEM22

polyclonal antibody, anti-HA high affinity (3F10) rat monoclonal antibody (Roche, Basel, Switzerland) or anti-Flag M2 monoclonal antibody (Sigma-Aldrich). Finally, the membranes were incubated with horseradish peroxidase (HRP) conjugated secondary antibody (Santa Cruz, CA, USA) and protein bands were visualized by enhanced chemiluminescence (ECL) detection reagents (GE Healthcare).

Immunocytochemical staining analysis. To examine the subcellular localization of TMEM22, COS7 cells were transiently transfected with HA- and Flag-tagged TMEM22 (pCAGGSn-HA-TMEM22-Flag) construct in a slide chamber (Laboratory-Tek II chamber slide; Nalgen Nunc International, Naperville, IL, USA) using FuGENE 6 reagent (Roche) according to the manufacturer's instructions. Forty-eight hours after transfection, cells were fixed with PBS (-) containing 4% paraformaldehyde for 15 min, and rendered permeable with PBS containing 0.1% Triton X-100 for 2.5 min at room temperature. Subsequently, the cells were covered with 3% BSA in PBS (-) at room temperature for 1 h to block non-specific hybridization, followed by incubation for 1 h with anti-HA antibody 3F10 (1:1000; Roche) and anti-Flag M2 antibody (1:1000; Sigma-Aldrich). After washing with PBS(-), the cells were double stained with Alexa 488-conjugated anti-rat (1:1000) and Alexa 594-conjugated anti-mouse fluorescent antibodies (1:1000) for 1 h (Molecular Probes, Eugene, OR). Nuclei were counterstained with 4',6'-diamidine-2'-phenylindole dihydrochloride (DAPI). Fluorescent images were obtained under a TCS SP2 AOBS microscope (Leica, Tokyo, Japan).

Effect of small-interfering RNA against TMEM22 or RAB37 on growth of RCC cells. We used siRNA oligonucleotides (Sigma-Aldrich Japan KK, Tokyo, Japan) due to its high transfection efficiency to further verify the knockdown effects of TMEM22 or RAB37. The sequences targeting each gene were as follows: siTMEM22 si#1; 5'-UGAGAUUGG ACAAUUCCAG-3', si#2; 5'-CUACAGUCUUCAGUGC CAU-3', siRAB37; 5'-GACUGGCAUGAAUGUGGAG-3', siEGFP; 5'-GCAGCACGACUUCUUCAAG-3'. Caki-1 or Caki-2 cells ($4x10^5$ cells in 6 cm dish for RT-PCR, $3x10^5$ cells in 6-well plate for protein extraction, $3x10^4$ cells in 12-well plate for MTT assay and $1x10^5$ cells in 6-well plate for colony formation assay) were transfected with 10 nM each of siRNAs using Lipofectamin RNAiMAX (Invitrogen, Carlsbad, CA) by reverse transfection method according to the instructions of manufacturer. Forty-eight hours after transfection, total RNAs were extracted from the transfected cells to evaluate knockdown effects by semi-quantitative RT-PCR. The specific primer sets for semi-quantitative RT-PCR are as follows; 5'-TGGCGATGATGGATATGAAG-3' and 5'-AGG GGGCCTCCTGATAGTAA-3' for *TMEM22*; 5'-TGAGGG CAGGTAATGACTCC-3' and 5'-GTGCTTGTGTGCTGG AGAAA-3' for RAB37; 5'-CATCCACGAAACTACCTT CAACT-3' and 5'-TCTCCTTAGAGAGAAGGGTG-3' for ß-actin as an internal control. Additionally, 72 h after transfection, we confirmed knockdown effect of TMEM22 at protein level by Western blot analysis with anti-TMEM22 antibody or ACTB antibody as a control. To quantify cell viability, 3-(4,5-dimethylthiazol-2-yl)-2,5-diphenyl-tetrazolium bromide (MTT) assay was performed with cell counting kit-8 (DOJINDO, Kumamoto, Japan) at 6 days after transfection according to manufacturer's recommendation. Absorbance at 490 nm wavelength was measured with a multilablel counter ARVO MX (Perkin Elmer, Boston, MA). These experiments were performed in triplicate. Moreover, 7 days after the transfection, the cells were fixed with 4% paraformaldehyde for 10 min and stained with Giemsa solution (Merck) to count the number of colonies.

Immunoprecipitation and mass spectrometry. To identify an interacting protein(s) with TMEM22 protein, HEK293 cells were plated onto 15 cm dishes ($3x10^6$ cells/dish, 16 dishes for each trasfection) and transfected with 20 μg of pCAGGSn-HA-TMEM22-Flag or pCAGGSnH3F-Mock (without insertion) using FuGENE6 reagent (Roche) according to the manufacturer's instructions. After 48-h incubation, the cells were lysed in IP-lysis buffer [50 mM Tris-HCl/150 mM NaCl/1% (w/v) CHAPS] including 0.1% protease inhibitor cocktail III (Calbiochem). The cell lysates were pre-cleaned with 1.2 μg of normal mouse IgG (Santa Cruz) and rec-Protein G Sepharose 4B (Zymed, San Francisco, CA) at 4˚C for 1 h. Subsequently, the lysates were incubated with anti-FLAG M2 agarose (Sigma-Aldrich) at 4˚C for 2 h. After washing 6 times with IP-washing buffer [50 mM Tris-HCl/150 mM NaCl/0.1% (w/v) CHAPS], proteins on beads were eluted with SDS-sample buffer incubated at 37˚C for 15 min and the proteins were separated in 10-20% SDS-PAGEs gels (Bio Ccraft, Tokyo, Japan). Proteins in polyacrylamide gel were silver stained by SilverQuest Silver Staining Kit (Invitrogen) according to the manufacturer's instructions. Bands that were specifically observed in the TMEM22-transfected lane were excised with a clean, sharp scalpel and the extracted proteins were applied for PMF (Peptide Mass Fingerprint) analysis using MALDI TOF-MS (Shimadzu Biotech, Tsukuba, Japan).

Co-immunoprecipitation assay. COS-7 cells were transiently transfected with pCAGGSn-TMEM22-HA and pCAGGSn-RAB37-Flag. Forty-eight hours after transfection, the cells were lysed with IP-lysis buffer as described in immuno-precipitation and mass spectrometry section. The cell lysates were pre-cleaned at 4˚C for 1 h, and subsequently incubated with monoclonal anti-HA-agarose antibody produced in mouse (Sigma-Aldrich) at 4˚C for 1 h. After washing with IP-lysis buffer, co-precipitated proteins were separated by SDS-PAGE. Finally, we performed Western blot analysis using anti-Flag M2 monoclonal antibody (Sigma-Aldrich) or anti-HA high affinity (3F10) rat monoclonal antibody (Roche) to detect the exogenously expressed-RAB37 or TMEM22 protein, respectively. Additionally, we performed co-immunoprecipitation with the same procedure using the cell lysates of COS7 cells which transiently transfected with pCAGGSn-TMEM22-Flag and pCAGGSn-RAB37-HA.

λ-phosphatase assay. To estimate the phosphorylation modification of RAB37, we performed λ protein phosphatase assay according to a previous report (11). Whole cell lysate of COS7 cells, which transfected with pCAGGSn-

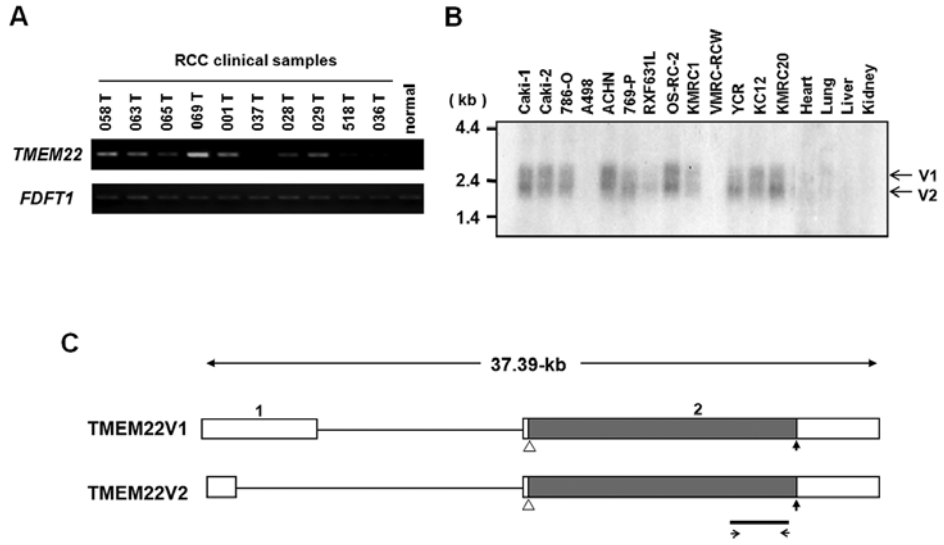

Figure 1. Expression of *TMEM22* in RCC and normal human tissues. (A) Expression of *TMEM22* in tumor cells (Cases, no. 058T, 063T, 065T, 069T, 001T, 037T, 028T, 029T, 518T and 036T) and normal renal cortex cells (normal) examined by semi-quantitative RT-PCR. Expression of *FDFT1* served as a quantity control. (B) Northern blot analysis of the *TMEM22* transcript in RCC cell lines (Caki-1, Caki-2, 786-O, A-498, ACHN, 769-P, RXF631L, OS-RC-2, KMRC1, VMRC-RCW, YCR, KC12 and KMRC20) and normal human organs (heart, lung, liver and kidney). (C) Genomic structure of two variants of TMEM22 (TMEM22V1 and TMEM22V2). Grey box indicates a coding region, and white boxes indicate non-coding regions. White triangles indicate initiation codon, and upward arrows indicate stop codon. The arrows indicate a primer set to examine expression of TMEM22. The line indicates the location of probe for Northern blot analysis. The number above each box indicates the exon number.

RAB37-HA, was incubated for 2 h at 30˚C in the presence or absence of 800 Units of λ protein phosphatase (New England Biolabs, Ipswich, MA). Subsequently, the protein samples were separated by SDS-PAGE and detected by Western blotting with anti-HA high affinity (3F10) rat monoclonal antibody (Roche).

Statistical analysis. Statistical significance was calculated by Student's t-test, using Excel software. A difference of $P<0.05$ was considered to be statistically significant.

Results

Identification of TMEM22 as a molecular target for RCC therapy. To screen molecular targets that could be applicable for development of novel therapeutic drugs, we previously performed genome-wide expression profile analysis of clear-cell renal cell carcinomas (RCC) by means of cDNA microarray representing 27,648 genes or ESTs (8). Among up-regulated genes, we focused on *TMEM22* as a novel molecular target for RCC therapy. Semi-quantitative RT-PCR experiments confirmed elevated expression of *TMEM22* in 7 of 10 RCC clinical samples (Fig. 1A). Subsequent Northern blot analysis confirmed that the two different transcripts of *TMEM22* were up-regulated in 9 of 13 RCC cell lines examined (Fig. 1B), while their expression was hardly detectable in 16 normal human tissues examined (data not shown).

In the NCBI database, cDNA sequences corresponding to two transcriptional variants, denoted as *TMEM22* isoform 1 (*TMEM22V1*) (GenBank accession number; NM_025246) and *TMEM22* isoform 2 (*TMEM22V2*) (GenBank accession number; NM_001097599), were deposited. The full-length cDNA sequences for *TMEM22V1* and *TMEM22V2* transcripts consist of 2079 and 1814 nucleotides, respectively.

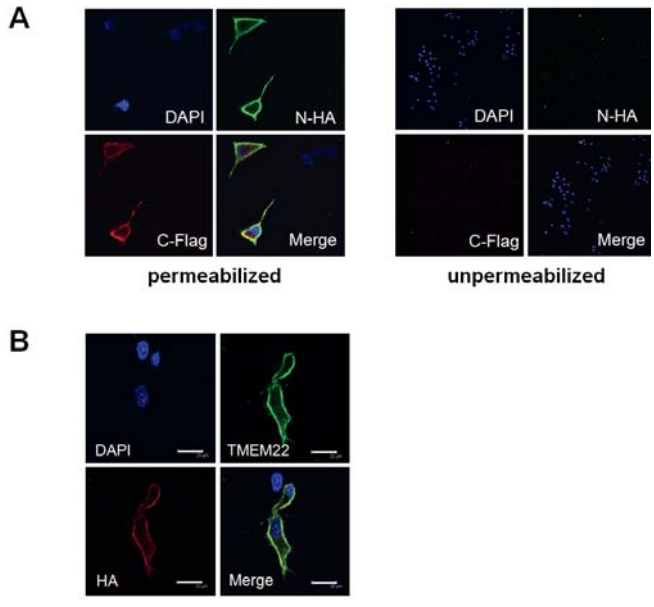

Figure 2. Subcellular localization of transiently expressed TMEM22 protein. (A) COS7 cells were transfected with N-terminal HA-tagged and C-terminal Flag-tagged TMEM22 (HA-TMEM22-Flag) construct. The cells were permeabilized with (left panel) and without (right panel) treatment of 0.1% Triton X-100, and immunocytochemically stained using anti-HA antibody (green), anti-Flag antibody (red) and DAPI (blue) to discriminate nucleus (see Materials and methods). (B) The transfected cells were double stained with anti-HA- and anti-TMEM22-specific antibodies after fixation and permeablization by Triton X-100.

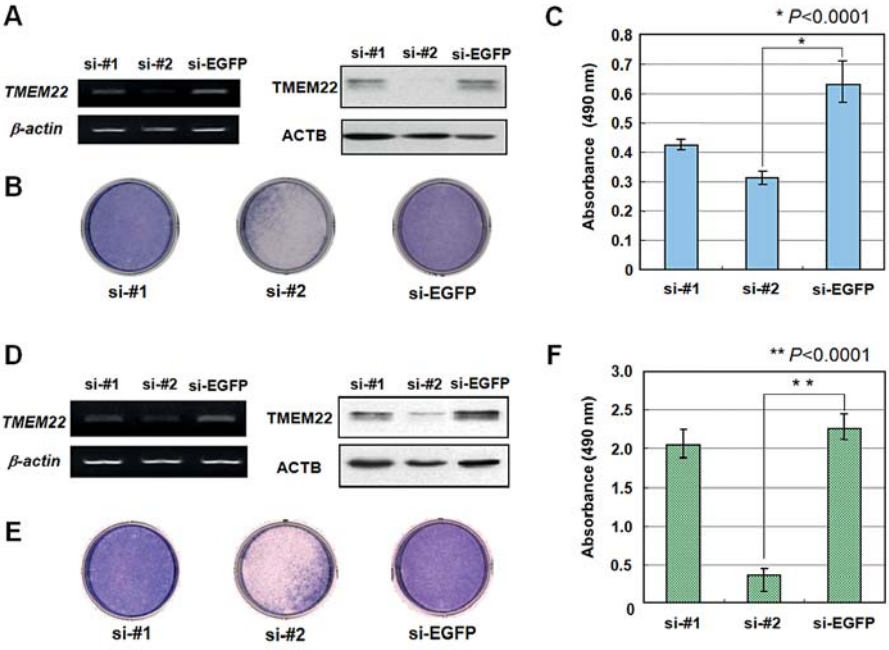

Figure 3. Growth-inhibitory effects of TMEM22 siRNAs to RCC cells. (A and D) Semi-quantitative RT-PCR and Western blot analyses showing suppression of endogenous expression of TMEM22 by TMEM22-specific siRNAs (si#1 and si#2) in RCC cell line, (A) Caki-2 and (D) -1. Expression of *β*-actin and ACTB served as a quantity control at transcriptional and protein levels, respectively. (B and E) Colony-formation assay demonstrating a decrease in the number of colonies by knockdown of TMEM22 in (B) Caki-2 and (E) -1 cells. (C) MTT assay demonstrating a decrease in the number of cells by knockdown of TMEM22 in Caki-2 cells (si-#2; p<0.0001; unpaired t test) and (F) Caki-1 cells (si-#2; p<0.0001; unpaired t test).

However, the two transcripts share the same open reading-frame, encoding a peptide of 412 amino acids. These two transcriptional variants consist of 2 exons, spanning an ~37-kb genomic region on the chromosomal band 3q22.3 (Fig. 1C). The PSORT II, SOSUI and the Simple Modular Architecture Research Tool (SMART) computer programs suggested the TMEM22 protein to have 10 transmembrane domains. A homology search of its amino-acid sequences in BLAST database identified several homologous proteins, including a *Canis familiaris* (XP_542795), a *Mus musculus* (NP_001094953), *Rattus norvegicus* (NP_001012126), a *Xenopus tropicalis* (NP_001096195) and a *Gallus gallus* protein (NP_001026470), which shared 97, 92, 91, 79 and 77% identity with TMEM22, respectively, indicating that this protein is highly conserved among species.

Subcellular localization of TMEM22 protein. We then investigated the sub-cellular localization of TMEM22 protein that was introduced into COS7 cells exogenously with an HA-tag at its N-terminus and also a Flag-tag at its C-terminus (HA-TMEM22-Flag). Since the TMEM22 protein was predicted to have 10 transmembrane domains, we examined whether the N- and C-terminus ends of this protein locate in the cytoplasmic side or the extracellular side. Immuno-cytochemical staining analysis with anti-HA-tag and anti-Flag-tag antibodies revealed that the two antibodies detected the exogenously introduced protein at the cytoplasmic membrane under the cell-permeabilized condition (Fig. 2A left panels), although no staining signal was detected under the cell-unpermeabilized condition (Fig. 2A, right panels). Hence, we suspected that N- and C-terminal regions of this protein were localized in the cytoplasm as predicted by *in silico* analysis. Furthermore, we confirmed its localization at the cytoplasmic membrane using anti-TMEM22 poly-clonal antibody that was generated using its N-terminal peptide (3-104 amino acids; see Materials and methods) (Fig. 2B).

Growth-inhibitory effects by small-interfering RNA (siRNA) against TMEM22. To assess the growth-promoting role of *TMEM22*, we knocked down the expression of endogenous *TMEM22* in RCC cell lines, Caki-2 and -1, in which *TMEM22* was overexpressed, using the TMEM22-specific siRNA oligonucleotides (see Materials and Methods). Semi-quantitative RT-PCR and Western blot analyses showed that TMEM22-specific siRNA (si-#2) suppressed TMEM22 expression at transcriptional and protein levels, as compared with a control siRNA (si-EGFP) as well as si-#1 (Fig. 3A and D). We then performed colony-formation (Fig. 3B and D) and MTT (Fig. 3C and F) assays and found that introduction of si-#2 remarkably suppressed growth of Caki-2 and -1 cells (Caki-2: si-#2, P<0.0001; Caki-1: si-#2, P<0.0001, Student's t-test), in concordance with the results of knock-down effect.

Identification of RAB37 as an interacting protein of TMEM22. Since the biological function of TMEM22 is totally unknown, we first searched for a protein(s) interacting with TMEM22 protein by immunoprecipitation and mass spectrometry analyses. Lysates of HEK293 cells transfected with a pCAGGSn-HA-TMEM22-Flag vector or a pCAGGSnH3F-Mock (mock control) were extracted, and

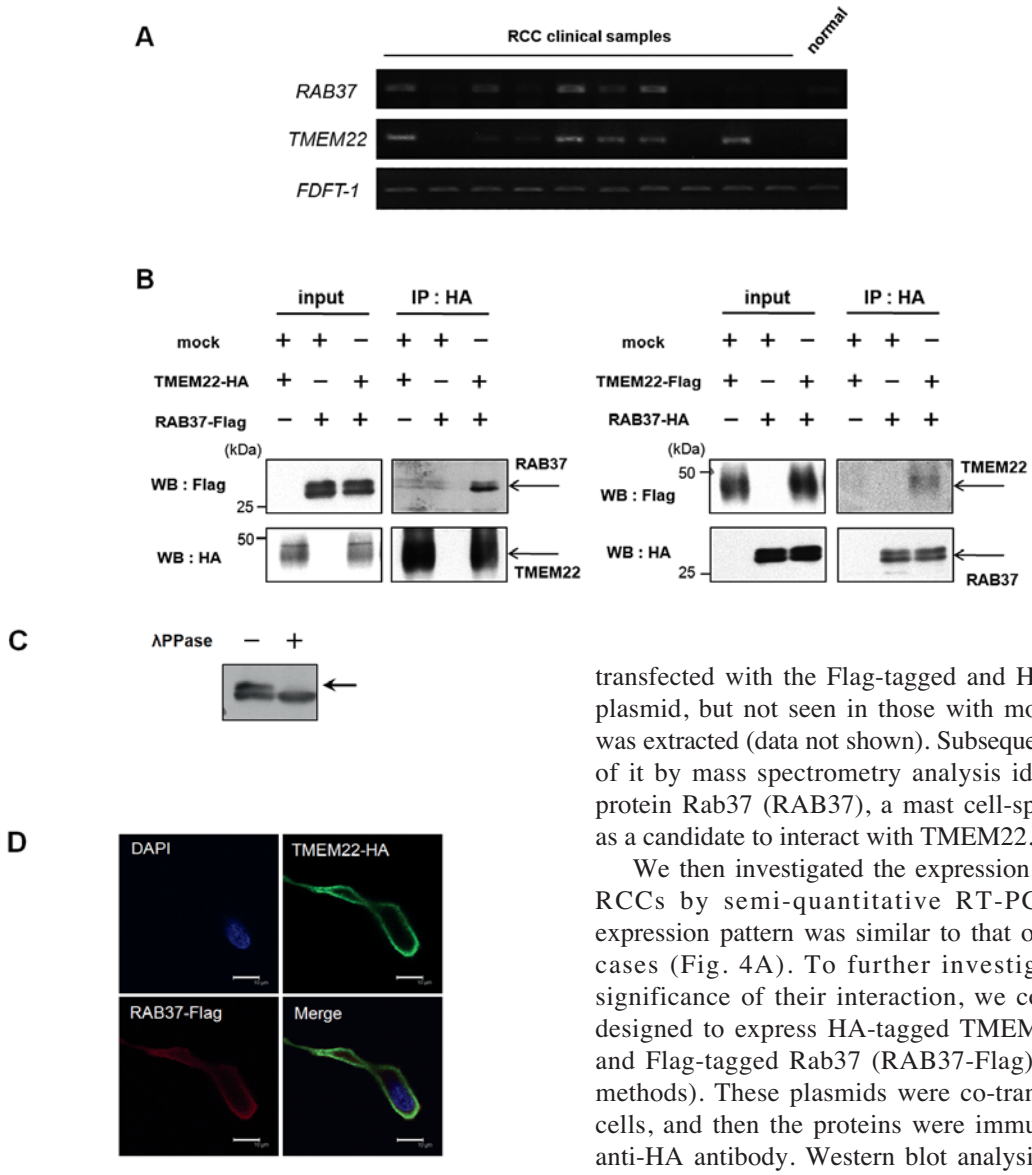

Figure 4. Interaction between TMEM22 and RAB37 proteins. (A) Expression of *TMEM22* and *RAB37* in clinical RCC cases and normal renal cortex (normal) by semi-quantitative RT-PCR. Expression of *FDFT-1* served as a quantity control. (B) Co-immunoprecipitation of TMEM22 and RAB37 proteins. Cell lysates from COS-7 cells transfected with HA-tagged TMEM22 (TMEM22-HA) and Flag-tagged RAB37 (RAB37-Flag) were immunoprecipitated with anti-HA antibodies. Immunoprecipitates were immunoblotted using monoclonal anti-HA or anti-Flag antibodies (left panels). Conversely, cell lysates from COS-7 cells transfected with Flag-tagged TMEM22 (TMEM22-Flag) and HA-tagged RAB37 (RAB37-HA) were immunoprecipitated with anti-HA antibodies. Immunoprecipitates were immunoblotted using monoclonal anti-HA or anti-Flag antibodies (right panels). (C) Phosphorylation of RAB37 protein. The cell lysates were incubated with or without λ-phosphatase (λ-PPase) for 2 h at 30˚C. A phosphorylated Rab37 protein was observed as a slowly migrated band as indicated by an arrow. (D) Co-localization of exogenous TMEM22 and RAB37 in COS7 cells. Exogenous TMEM22 protein (green) co-localized exogenous Rab37 protein (red) under the cytoplasmic membrane of COS7 cells. Scale bar, 10 μm.

immunoprecipitated with anti-Flag M2 monoclonal antibody (see Materials and methods). Protein complexes were silver-stained on 10-20% SDS-PAGE gels. A protein, which was seen in immunoprecipitates of lysates prepared from the cells transfected with the Flag-tagged and HA-tagged TMEM22 plasmid, but not seen in those with mock control plasmid, was extracted (data not shown). Subsequent peptide sequences of it by mass spectrometry analysis identified Ras-related protein Rab37 (RAB37), a mast cell-specific GTPase (20), as a candidate to interact with TMEM22.

We then investigated the expression levels of RAB37 in RCCs by semi-quantitative RT-PCR, and found its expression pattern was similar to that of TMEM22 in RCC cases (Fig. 4A). To further investigate the biological significance of their interaction, we constructed plasmids designed to express HA-tagged TMEM22 (TMEM22-HA) and Flag-tagged Rab37 (RAB37-Flag) (see Materials and methods). These plasmids were co-transfected into COS-7 cells, and then the proteins were immunoprecipitated with anti-HA antibody. Western blot analysis of the precipitates using anti-Flag antibody indicated that TMEM22-HA was co-precipitated with RAB37-Flag (Fig. 4B; left panel). Conversely, we constructed the Flag-tagged TMEM22 (TMEM22-Flag) and HA-tagged RAB37 (RAB37-HA), and performed immunoprecipitation using anti-HA antibody and subsequent Western blot analysis of the precipitates using anti-Flag antibody. The results also showed that TMEM22-Flag was co-precipitated with RAB37-HA (Fig. 4B; right panel). Moreover, we detected an additional band of RAB37 with high molecular weight in the co-immunoprecipitation experiment with the TMEM22 protein. We confirmed the high molecular-weight band had disappeared after treatment of λ phosphatase (Fig. 4C), suggesting that TMEM22 protein interacted with the phosphorylated form of RAB37 as well as unphosphorylated form.

We also performed immunocytochemical analysis of TMEM22 and RAB37 in mammalian cells. The TMEM22-HA and RAB37-Flag constructs were transfected into COS7 cells according to the procedure as described in Materials and methods. The results revealed the partially-overlapped localization of exogenously expressed TMEM22-HA and RAB37-Flag under the cytoplasmic membrane in the transfected cells (Fig. 4D).

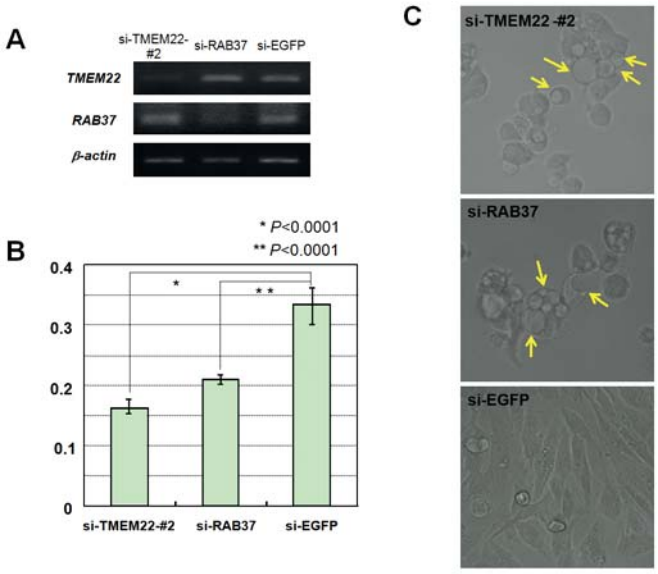

Figure 5. Effect of TMEM22 and RAB37 on proliferation of RCC cells. (A) Effect of *TMEM22* and *RAB37* siRNAs on Caki-1 cells analyzed by semi-quantitative RT-PCR. Expression of ß-actin served as a quantity control. (B) MTT assays demonstrating a decrease in the number of cells by knockdown of TMEM22 or RAB37 in Caki-1 cells (si-TMEM22-si#2; p<0.0001, si-RAB37; p<0.0001; unpaired t-test). (C) Observation of morphological changes of Caki-1 cells transfected with si-TMEM22 or si-RAB37 by microscope. si-EGFP was used as a control. The arrowheads indicate round shapes and vacuolization in cytoplasm of si-TMEM22 and si-RAB37-transfected cells (yellow arrows).

Growth-inhibitory effects of RAB37-specific siRNA in RCC. To further validate the biological significance of RAB37 in renal carcinogenesis, we designed the *RAB37*-specific siRNA oligonucleotide, and examined the knockdown effect of siRNA in Caki-1 cell line, which overexpressed *TMEM22* and *RAB37* (data not shown). Semi-quantitative RT-PCR detected knockdown effects by si-TMEM22-#2 and si-Rab37 on their expression (Fig. 5A). A subsequent MTT assay revealed that introduction of si-TMEM22-#2 or si-RAB37 into in Caki-1 cells resulted in the significant decrease of the cell viability, compared with a control EGFP-siRNA (Fig. 5B). Interestingly, introduction of either TMEM22- or RAB37-specific siRNA into the Caki-1 cells caused a similar morphological change of the cells; the cells became a round shape and revealed vacuolization (Fig. 5C), indicating that *TMEM22* and *RAB37* are essential for the growth of RCC cells.

Discussion

Significant advances in development of molecular-targeting drugs for cancer therapy have been achieved in the last two decades. However, the proportion of patients showing good response to presently available treatments is still very limited and a subset of the patients suffers from severe adverse reactions without any benefit (2-5). Hence, it is urgent to develop new anticancer agents that are highly specific to malignant cells, with a minimum risk of adverse reactions. Through the detailed expression profile analysis of clear-cell types of RCC, we identified *TMEM22* to be significantly overexpressed in majority of RCC cases. Subsequent Northern blot analysis revealed its hardly-detectable level of expression in the normal human tissues examined.

TMEM22 gene encodes a putative 421-amino-acid protein that is predicted to contain 10 transmembrane domains and is highly conserved among species by *in silico* analysis. We demonstrated experimentally that TMEM22 protein was localized at the cytoplasmic membrane in mammalian cells, and its N- and C-terminal regions were present at the cytoplasmic side in concordance with the *in silico* prediction. Furthermore, depletion of *TMEM22* expression by means of siRNA treatment drastically suppressed cell growth of RCC. However, since introduction of TMEM22 into COS7 cells could not enhance the growth of the cells (data not shown), we assume that TMEM22 is essential for the survival of RCC cells, but not sufficient enough to enhance the cell growth. These results implied that TMEM22 could serve as a valuable target for development of anti-cancer agents, especially therapeutic antibodies for RCC.

As described above, the biological functions of TMEM22 protein is totally unknown. Hence, to elucidate the biological significance of TMEM22 in RCC cells, we searched its interacting protein(s) and identified RAB37 protein, that was previously isolated as a novel mast cell-specific GTPase (18), as a candidate. *In silico* analysis predicted that RAB37 contained an important motif for guanine nucleotide binding, that are highly conserved among other low molecular-weight GTPases. Moreover, it contained the highly conserved cysteine residues for isoprenylation, especially the motif for geranylgeranyl addition, which is essential for the membrane association, implying that RAB37 may be a cytoplasmic membrane-anchored protein for TMEM22. As shown in Fig. 4, we demonstrated *in vivo* interaction of TMEM22 and RAB37 and their co-localization in mammalian cells. These findings suggest that a TMEM22/RAB37 complex might function as small GTPase under the cytoplasmic membrane in RCC cells.

To assess whether TMEM22 or RAB37 plays a critical role in growth or survival of RCC cells, we knocked down the expression of endogenous TMEM22 and RAB37 in a RCC cell line, Caki-1, that expressed high levels of TMEM22 and RAB37, using siRNA specific to these molecules. Each of the specific siRNAs effectively suppressed their expression level, and resulted in the significant growth suppression of the Caki-1 cells, indicating that TMEM22 and RAB37 are essential for the growth of RCC cells. We also observed some morphological alterations such as vacuolization in cells treated with RAB37-siRNA as similar as those treated with TMEM22-siRNA. Since inhibition of their interaction may lead to cell death in RCC cells, the inhibitor for their interaction would be a possible valuable target to develop agents against RCC. Although further analysis of the function of TMEM22 will be necessary, the results provided here should contribute to more profound understanding of renal carcinogenesis and to development of novel therapies for RCCs.

Acknowledgements

We thank Dr Makoto Fujime of Juntendo University School of Medicine for collecting RCC tissue samples and their clinical

information, Ms Yoshiko Fujisawa for grateful technical supports and Drs Chikako Fukukawa, Yosuke Harada, Jae-Hyun Park and Meng-Lay Lin for helpful discussions.

References

1. Parkin DM, Bray F, Ferlay J and Pisani P: Global Cancer Statistics, 2002. CA Cancer J Clin 55: 74-108, 2005.
2. Cohen HT and McGovern FJ: Renal-cell carcinoma. N Engl J Med 353: 2477-2490, 2005.
3. Lane BR, Rini BI, Novick AC and Campbell SC: Targeted molecular therapy for renal cell carcinoma. Urology 69: 3-10, 2007.
4. Costa LJ and Drabkin HA: Renal cell carcinoma: new developments in molecular biology and potential for targeted therapies. Oncologist 12: 1404-1415, 2007.
5. Rini BI, Rathmell WK and Godley P: Renal cell carcinoma. Curr Opin Oncol 20: 300-306, 2008.
6. Petricoin EF 3rd, Hackett JL, Lesko LJ, Puri RK, Gutman SI, Chumakov K, Woodcock J, Feigal DW Jr, Zoon KC and Sistare FD: Medical applications of microarray technologies: a regulatory science perspective. Nat Genet 32: 474-479, 2002.
7. Togashi A, Katagiri T, Ashida S, Fujioka T, Maruyama O, Wakumoto Y, Sakamoto Y, Fujime M, Kawachi Y, Shuin T and Nakamura Y: Hypoxia-inducible protein 2 (HIG2), a novel diagnostic marker for renal cell carcinoma and potential target for molecular therapy. Cancer Res 65: 4817-4826, 2005.
8. Hirota E, Yan L, Tsunoda T, Ashida S, Fujime M, Shuin T, Miki T, Nakamura Y and Katagiri T: Genome-wide gene expression profiles of clear cell renal cell carcinoma: Identification of molecular targets for treatment of renal cell carcinoma. Int J Oncol 29: 799-827, 2006.
9. Kanehira M, Katagiri T, Shimo A, Takata R, Shuin T, Miki T, Fujioka T and Nakamura Y: Oncogenic role of MPHOSPH1, a cancer-testis antigen specific to human bladder cancer. Cancer Res 67: 3276-3285, 2007.
10. Kanehira M, Harada Y, Takata R, Shuin T, Miki T, Fujioka T, Nakamura Y and Katagiri T: Involvement of upregulation of DEPDC1 (DEP domain containing 1) in bladder carcinogenesis. Oncogene 26: 6448-6455, 2007.
11. Park JH, Lin ML, Nishidate T, Nakamura Y and Katagiri T: PDZ-binding kinase/T-LAK cell-originated protein kinase, a putative cancer/testis antigen with an oncogenic activity in breast cancer. Cancer Res 66: 9186-9195, 2006.
12. Shimo A, Nishidate T, Ohta T, Fukuda M, Nakamura Y and Katagiri T: Elevated expression of protein regulator of cytokinesis 1, involved in the growth of breast cancer cells. Cancer Sci 98: 174-181, 2007.
13. Lin ML, Park JH, Nishidate T, Nakamura Y and Katagiri T: Involvement of maternal embryonic leucine zipper kinase (MELK) in mammary carcinogenesis through interaction with Bcl-G, a pro-apoptotic member of Bcl-2 family. Breast Cancer Res 9: R17, 2007.
14. Shimo A, Tanikawa C, Nishidate T, Lin ML, Matsuda K, Park JH, Ueki T, Ohta T, Hirata K, Fukuda M, Nakamura Y and Katagiri T: Involvement of kinesin family member 2C/mitotic centromere-associated kinesin overexpression in mammary carcinogenesis. Cancer Sci 99: 62-70, 2008.
15. Ueki T, Nishidate T, Park JH, Lin ML, Shimo A, Hirata K, Nakamura Y and Katagiri T: Involvement of elevated expression of multiple cell-cycle regulator, DTL/RAMP (denticleless/RA-regulated nuclear matrix associated protein), in the growth of breast cancer cells. Oncogene (In press).
16. Rozsa FW, Scott KM, Pawar H, Samples JR, Wirtz MK and Richards JE: Differential expression profile prioritization of positional candidate glaucoma genes: the GLC1C locus. Arch Ophthalmol 125: 117-127, 2007.
17. Katagiri T, Ozaki K, Fujiwara T, Shimizu F, Kawai A, Okuno S, Suzuki M, Nakamura Y, Takahashi E and Hirai Y: Cloning, expression and chromosome mapping of adducin-like 70 (ADDL), a human cDNA highly homologous to human erythrocyte adducin. Cytogenet Cell Genet 74: 90-95, 1996.
18. Masuda ES, Luo Y, Young C, Shen M, Rossi AB, Huang BC, Yu S, Bennett MK, Payan DG and Scheller RH: Rab37 is a novel mast cell specific GTPase localized to secretory granules. FEBS Lett 470: 61-64, 2000.